ACS SyntheticBiology

pubs.acs.org/synthbio

Research Article

Homologous Quorum Sensing Regulatory Circuit: A Dual-Input Genetic Controller for Modulating Quorum Sensing-Mediated Protein Expression in *E. coli*

Pricila Hauk, Kristina Stephens, Chelsea Virgile, Eric VanArsdale, Alex Eli Pottash, John S. Schardt, Steven M. Jay, Herman O. Sintim, and William E. Bentley*

Cite This: *ACS Synth. Biol.* 2020, 9, 2692–2702

Read Online

ACCESS | Metrics & More | Article Recommendations | Supporting Information

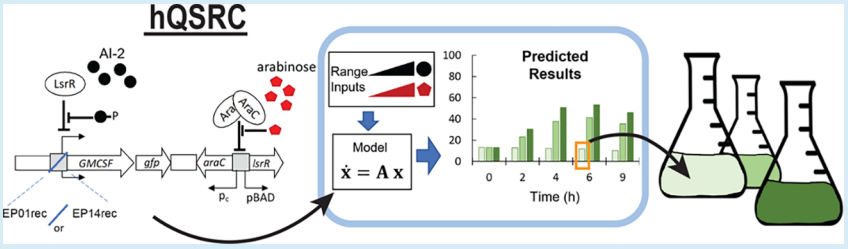

ABSTRACT: We developed a hybrid synthetic circuit that co-opts the genetic regulation of the native bacterial quorum sensing autoinducer-2 and imposes an extra external controller for maintaining tightly controlled gene expression. This dual-input genetic controller was mathematically modeled and, by design, can be operated in three modes: a constitutive mode that enables consistent and high levels of expression; a tightly repressed mode in which there is very little background expression; and an inducible mode in which concentrations of two signals (arabinose and autoinducer-2) determine the net amplification of the gene(s)-of-interest. We demonstrate the utility of the circuit for the controlled expression of human granulocyte macrophage colony stimulating factor in an engineered probiotic *E. coli*. This dual-input genetic controller is the first homologous AI-2 quorum sensing circuit that has the ability to be operated in three different modes. We believe it has the potential for wide-ranging biotechnological applications due its versatile features.

Reprogramming metabolic and biosynthetic functions within microorganisms enables both new routes for biopharmaceuticals production,[1] and more recently, for the diagnosis and treatment of disease.[2−13] The terms "smart bacteria" or "smart probiotics" have been used to describe the latter, reprogrammed bacteria that make decisions based on prevailing molecular cues and that subsequently take action, including expressing a marker protein as an indicator of disease and/or a small molecule or protein-based therapeutic for treatment.[13−20] Several environmental conditions such pH, oxygen tension, and host inflammatory conditions, or even the absence of an important nutrient, have the potential to be used for signaling these bacteria.[7,21−25] That is, because there is now an extensive network of signal/receptor pairs that enable tight exogenous control of gene regulation,[26] many gene circuits have appeared that ensure high signaling fidelity and precise control of the intended bacterial program. For example, bacterial community size has served as a factor, wherein a quorum-sensing (QS) signal molecule, indicating the presence of a number of pathogens, was used to signal the synthesis and delivery of a pathogen-specific toxin from an engineered commensal strain.[3] In addition, microfluidic systems that recapitulate QS activity *in vitro* have appeared[27−31] along with mathematical models of quorum sensing;[32−37] these enable design and characterization of engineered strains. Accordingly, QS systems and their components are widely exploited for building circuits that help to detect metabolic diseases, fight bacterial infections, or serve as biosensors. QS component libraries have served in this capacity as repositories for subsequent assembly of a variety of useful circuits.[18,38−40]

The autoinducer-1 (AI-1) family of autoinducers, also called acyl-homoserine lactones (AHL), mediates intraspecies communication, including signaling among pathogenic strains enabling their detection in native environments. AI-1 systems have also been assembled into heterologous synthetic circuits. Because there are no AI-1 receptor/synthase pair homologues in *E. coli*, these bacteria do not natively respond to AI-1. Thus, there are few off target responses that might otherwise alter the phenotype in unintended directions. When paired with the

Received: April 1, 2020
Published: August 21, 2020

https://dx.doi.org/10.1021/acssynbio.0c00179
ACS Synth. Biol. 2020, 9, 2692–2702

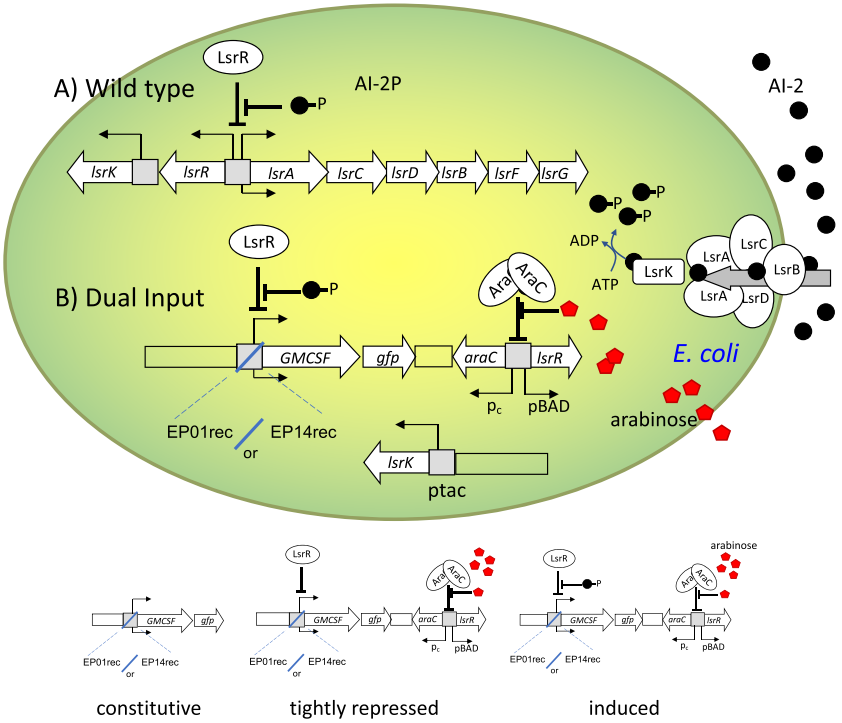

Figure 1. Schematic of dual-input genetic controller for modulating quorum sensing (QS)-mediated protein expression. (A) QS genetic regulation in *E. coli*. Lsr operon is regulated by LsrR (repressor), LsrK (AI-2 kinase), and AI-2 (inducer, produced *via* LuxS). (B) Homologous quorum sensing regulatory circuit (hQSRC). The hQSRC system consists of two parts: pPHT01 or pPHT14 (Plasmid #1) and pSkunk-*lsrK* (Plasmid #2). pPHT01 and pPHT14 harbor evolved *lsr* promoters, EP01rec and EP14rec,[57] respectively. The *araC-pBAD-lsrR* sequence was introduced to provide extra LsrR repression by arabinose addition. The second plasmid is a p15a origin plasmid expressing LsrK under the *tac* promoter basal levels.

knowledge that AI-1 freely diffuses through *E. coli* membranes, this attribute enables the incorporation of a variety of pathogen-specific components that provide for sophisticated engineered circuits (for instance, multi-input circuits[41−43]) and pathogen-targeting functions.[39]

On the other hand, autoinducer-2 (AI-2) is an interkingdom signaling molecule[44] produced and/or sensed by many bacterial species, including Gram positive species and commensal Gram negative strains,[18] as well as pathogens.[45] In *E. coli*, QS is regulated by the *lsr* promoter *via* AI-2 (signal) and its cognate repressor, LsrR. Because the native *lsr* promoter is subject to interference by several *E. coli* global regulators (*e.g.*, CRP and σ^s) and is a relatively weak promoter,[46−51] its use in synthetic systems has been limited. Instead, AI-2 QS circuitry enables native signaling processes to be coopted for specific user-intended purposes wherein the endogenous phenotypes are meant to be exploited or augmented (*e.g.*, autoinduction of heterologous proteins,[51] or programmed chemotaxis[52]).

Seeking to expand the use of native bacterial communication within the biotechnology arena, our group focused here on the development of an homologous synthetic circuit based on *E. coli* AI-2 QS. We had previously modeled the AI-2 system using several methods including a population-based study of emergent behavior including chemotaxis,[32] a spatially resolved agent-based approach,[53] a metabolically detailed stochastic Petri Net approach,[54] and the more typical ODE methods aimed at revealing intracellular circuit design[55] or optimizing[34] AI-2 uptake. In this work, we created a simple gene circuit model to characterize our previous efforts that enabled tuned responses based on altered repression.[56,57] Specifically, we had evolved the *lsr* promoter, creating a library containing stronger *lsr* promoter variants, EP01rec and EP14rec.[57] These two mutated promoters were 8-fold stronger than the wild type and yet retained the native LsrR repressor function when the promoters were provided on low copy vectors (∼1−2 copies). In this work, we have employed these variants in dual-input genetic controllers for modulating QS networks wherein the wildtype LsrR expression level is augmented by the arabinose-activated pBAD promoter. In addition, LsrK kinase was incorporated into the system to maintain heightened levels of phosphorylated AI-2. The system thus consists of two plasmids, pPHT01 or pPHT14, and pSkunk-LsrK. The pPHT01 and pPHT14 plasmids carry the evolved *lsr* promoters, EP01rec and EP14rec, respectively, for driving a gene-of-interest and *lsrR* expression placed under the pBAD promoter (Figure 1). A simple ODE-based model, based on typical repressor/activator functions, enables quantification of both the degree of repression and activation that should be obtained. That is, the controller exhibits tunable repression owing to arabinose-inducible LsrR under the pBAD promoter, and induction by AI-2 using the evolved *lsr* promoters, EP01rec and EP14rec. The circuit also shows efficient constitutive expression in the absence of arabinose.

This new system denoted the "homologous quorum sensing regulatory circuit" (hQSRC) is based on native *E. coli* quorum sensing and has the potential for a variety of metabolic engineering and synthetic biology applications, especially where native interspecies communication is envisioned. For example, biomolecule conversion or production using cocultures[58−61] or consortia[62,63] may benefit from such a system. Additionally, cell constructs intentionally deployed in

https://dx.doi.org/10.1021/acssynbio.0c00179
ACS Synth. Biol. 2020, 9, 2692−2702

complex environments where exogenous control may be difficult, such as smart probiotics or those that are based on interkingdom signaling, may benefit. We anticipate a variety of applications in a variety of settings.

MATERIALS AND METHODS

Strains and Media. DH5α (NEB), PH04, and PH08 strains (Supplementary Table S1) were grown in Luria−Bertani (LB) medium at 37 °C for DNA manipulation or expression experiments. Media were supplemented with chloramphenicol (34 μg/mL) to maintain pPHT, pPHT01, pPHT14, pPHT01-YebF-rhGM-CSF, and pPHT14-YebF-rhGM-CSF, kanamycin (25 μg/mL) for pBAD-*lsrR*, spectinomycin (25 μg/mL) for pSkunk-*lsrK*, and ampicillin (50 μg/mL) to maintain pAES40 (AthenaES), pAES40-GM-CSF or pGM29OmpA (Sletta *et al.* 2007)[66] plasmids (Supplementary Table S1).

***E. coli* Knockouts.** PH04 and PH08 are derived from *E. coli* LW7 and *E. coli* Nissle (EcN), respectively. The *ptsH* gene was deleted from both LW7 and EcN. The *luxS* gene was also knocked out from the EcN genome. Homologous recombination facilitated by λ Red recombinase was used to construct knockouts.[64] The pKD3 plasmid was used as template for PCR, and the ptsHd_Fw and ptsHd_Rv primers were used to create the PH04 strain, while luxSEcN_Fw, luxSEcN_Rv, HprEcN_Fw, and HprEcN_Rv were used to create the PH08 strain. Deletion of *ptsH* and *luxS* genes was confirmed by PCR. The pCP20 plasmid was used for removing the antibiotic cassettes from the genome.[65] Primer sequences are listed in Supplementary Table S2.

Plasmid Construction. pPHT, pPHT01, and pPHT14 are derived from plasmids pLSR, pLSR01 and pLSR14, respectively. pLSR, pLSR01, and pLSR14 contain *gfpmut2* under *lsr* promoter variant, either wild type, EP01rec, or EP14rec, respectively.[57] pPHT, pPHT01, and pPHT14 also contain *araC*-pBAD-*lsrR*. To construct these plasmids, *lsrR* was first cloned into pBAD/HisA (Invitrogen) to create pBAD-*lsrR*. The *araC*-pBAD-*lsrR* sequence (2264 bp) was then amplified through PCR using pBAD-*lsrR* as a template. The *araC*-pBAD-*lsrR* fragment was inserted into pLSR, pLSR01, and pLSR14, creating plasmids pPHT, pPHT01, and pPHT14.

pPHT01-*yebF*-rhGM-CSF and pPHT14-*yebF*-rhGM-CSF are derived from pPHT01 and pPHT14 and contain the *yebF*-rhGM-CSF-His6 (rhGM-CSF chimera) sequence downstream of the *lsr* promoter (either EP01rec or EP14rec) and upstream of *gfpmut2*. To construct the *yebF*-rhGM-CSF-His6 sequence, pGM29OmpA[66] was used as a template for amplifying the rhGM-CSF sequence. This was then cloned into pAES40 (AthenaES) containing *yebF*. pAES40-rhGM-CSF was then used as a template to amplify the *yebF*-rhGM-CSF-His6 fragment for cloning into pPHT01 and pPHT14. The *yebF*-rhGM-CSF-His6 insert was ligated into pPHT01 and pPHT14.

The *lsrK* gene was amplified from *E. coli* genome and cloned into the pSkunk plasmid. Plasmid information and primer sequences are also available in Supplementary Table S1 and Supplementary Table S2, respectively.

Repression and Induction Experiments. PH04 harboring hQSRCwt, hQSRC01, or hQSRC14 were grown overnight at 37 °C in 2 mL of LB medium supplemented with 25 μg/mL of spectinomycin and 34 μg/mL of chloramphenicol. Bacterial suspensions were then reinoculated into 10 mL of fresh LB medium with chloramphenicol and spectinomycin in order to have initial optical densities ($OD_{600\ nm}$) of 0.05.

To evaluate the pBAD-*lsrR* system repression range over the wild-type *lsr* promoter, EP01rec and EP14rec promoters,[57] 0.002, 0.02, and 0.2% arabinose were added to the cultures. Cells were allowed to grow in duplicate cultures at 37 °C with shaking at 250 rpm. Bacterial cell samples (200 μL, technical triplicate) were collected at optical density ($OD_{600\ nm}$) ∼ 0.2, and after 2 and 4 h of additional cell growth.

To analyze the derepression caused by AI-2 over the wild-type *lsr* promoter and its variants, experiments were conducted adding synthetic AI-2 in the absence or presence of 0.005 and 0.01% arabinose. At $OD_{600\ nm}$ ∼ 0.2 cultured cells were induced by adding 0, 40, or 80 μM of synthetic AI-2. Cells were collected at $OD_{600\ nm}$ ∼ 0.2 (induction start point) and after 2, 4, 6, and 9 h.

To prepare samples for analysis of GFP expression, samples were centrifuged (1000*g*, 5 min), washed, resuspended in 1× PBS, and kept on ice until flow cytometry. Results are the averages of analytical triplicates and duplicate experiments.

GFP Expression. Flow cytometry analyses were performed using a FACSCanto II flow cytometer equipped with 488, 633, and 405 nm lasers (BD Biosciences, San Jose, CA) and all flow cytometry data were analyzed with FACSDiva software (BD Biosciences). Side and forward scatter of bacterial suspensions were determined using semilog scale SSC/FSC plots with a threshold of 5000. Voltage settings for the SSC, FSC, and FITC channels were kept constant for all flow cytometry experiments. Bacterial suspensions were analyzed at a medium flow rate with a maximum of 1000 events per second for 75 s and a minimum of 50 000 events. Positive cells for GFP fluorescence were compared with negative controls (LW6 pLSR14 and *E. coli* W3110).

Human GM-CSF (hGM-CSF) Expression Experiments. *E. coli* Nissle PH08 harboring hQSRC01 rhGM-CSF chimera were grown overnight at 37 °C in 2 mL of LB medium supplemented with 25 μg/mL of spectinomycin and 34 μg/mL of chloramphenicol. Cells were reinoculated into 15 mL of fresh LB medium supplemented with antibiotics mentioned above in the same concentrations. Repression and induction were evaluated based on the presence or absence of either 0.01% arabinose and/or 40 μM synthetic AI-2. Cells were grown at 37 °C with shaking at 250 rpm for 4 h. Cultures were then centrifuged (5000*g*, 10 min). Cell-free supernatant fractions were precipitated overnight with 10% TCA at 4 °C. After centrifugation at 10 000 rpm for 10 min the pellet was washed once with ice-cold 100% acetone. All samples were resuspended in 70 μL of 2× SDS-PAGE buffer to be analyzed by Western Blot.

Western Blot Analysis. To detect rhGM-CSF chimera excreted into the PH08 culture media, supernatant from different conditions were precipitated using the TCA method as described above. After that, samples were loaded in equal volumes of 2× SDS-buffer for separation on 15% SDS-PAGE gel and then transferred to a PVDF membrane for Western blot analysis. To detect rhGM-CSF chimera a polyclonal rabbit anti-YebF (1:20 000, AthenaES) was used. Membranes were developed using SuperSignal West Femto Maximum Sensitivity Substrate according to the manufacturer's instructions.

Protein Purification. The rhGM-CSF chimera was expressed under the constitutive expression mode (in absence of both arabinose and AI-2) and purified from PH08 cell-free supernatant after 4 h of growth. Supernatant was absorbed to

https://dx.doi.org/10.1021/acssynbio.0c00179
ACS Synth. Biol. 2020, 9, 2692−2702

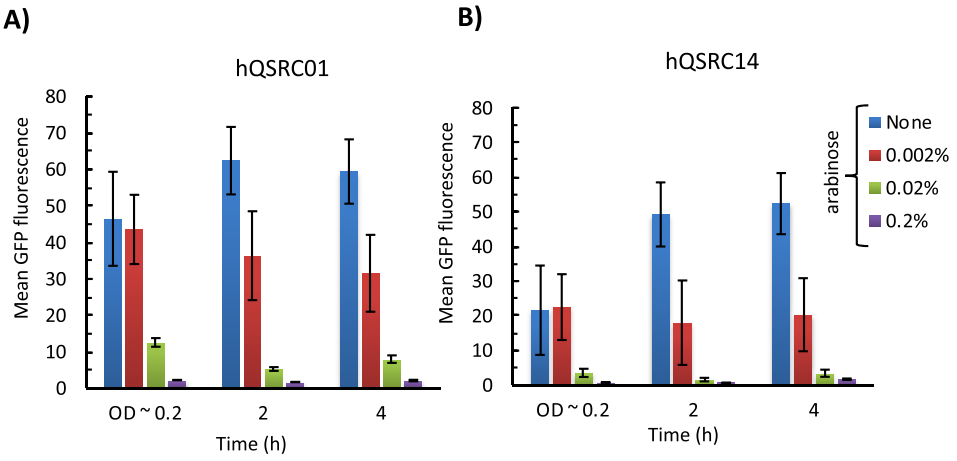

Figure 2. Representative FACS histograms show the mean GFP fluorescence from *E. coli* PH04 (Δ*luxS* Δ*ptsH*) cells transformed with hQSRC01 (A) or hQSRC14 (B) (see Figure 1). Panels (A) and (B) show arabinose dose-dependent repression. PH04 were grown in LB media until $OD_{600\ nm}$ ~ 0.2 and then supplemented with 0, 0.002, 0.02, and 0.2% arabinose and shaken at 37 °C for 2 and 4 h. GFP expression was measured at three different points, $OD_{600\ nm}$ of 0.2 (starting point), 1.0 (2 h), and ~2.5 (4 h). Data are plotted as means ± standard deviations of technical triplicates.

HiTrap Chelating HP filled with 1 mL of Ni^{2+}-charged chelating Sepharose (GE Healthcare) previously equilibrated with PBS 1×, pH 7.4 buffer. After absorption of rhGM-CSF chimera, the resin was washed with 5 volumes of PBS 1×, pH 7.4 containing 5 mM imidazole, following protein elution with 5 volumes of PBS 1×, pH 7.4 containing 150 mM imidazole. The purified rhGM-CSF chimera was dialyzed against PBS 1×, pH7.4 buffer and then concentrated to 100 μg/mL to have its activity tested in the human erythroleukemia cell line (TF-1).

Recombinant hGM-CSF Activity. *Cell Lines and Reagents.* The TF-1 cell line was obtained from Dr. David Stroncek (National Cancer Institute). TF-1 cells were maintained in RPMI 1640 (ATCC) with 10% FBS, 1% Pen-Strep, and 2 ng/mL recombinant human GM-CSF (Pepro-Tech).

Cell Proliferation Assays. TF-1 cells were seeded at 20 000 cells per well, in media supplemented with 10% FBS, 1% Penicillin−Streptomycin, in a 24 well plate (VWR 10062−900), treated with rhGM-CSF chimera (0.01−1000 ng/mL) or GM-CSF (PeproTech) used as a control, incubated in 5% CO_2 at 37 °C for 4 days, and analyzed using Alamar Blue (Bio-Rad) following the manufacturer's protocol.

Analysis of Activity. Each data set was fit to a logistic curve to determine EC50, the concentration at which half maximal activity occurs. The best fit value for EC50 along with 95% confidence bounds (lower and upper) were determined using the MATLAB (Version R2016a) curve fitting tool with the "nonlinear least squares" fit method.

Mathematical Model. The model consists of 11 ordinary differential equations (ODEs) that describe both the AI-2 QS components native to the host and the additional components introduced by the hQSRC. The equations were solved in MATLAB Version R2016a using the ODE45 solver. Additional details are provided in Supplementary Note S1.

RESULTS AND DISCUSSION

AI-2 Synthetic Circuit: Parts and Strain Engineering. Figure 1 depicts the native *E. coli* QS circuitry (Figure 1A) and our dual-input QS regulator for controlling homologous quorum sensing (Figure 1B) that is comprised of three parts: (i) an *lsr* or *lsr*-derived promoter (EP01rec or EP14rec); (ii) the LsrR repressor expressed *via* a non-QS signaling modality (*e.g.*, under pBAD promoter); and (iii) the Lsr kinase, LsrK, which enables enhanced sensitivity to AI-2[67,68] (*e.g.*, expressed *via* pSkunk-*lsrK* which has a p15a origin of replication and expresses LsrK kinase under the uninduced *tac* promoter). These components provide for tunable control of heterologous gene expression *via* native AI-2 QS signaling. We refer to this system as an homologous quorum sensing regulatory circuit (hQSRC) and have constructed two testable examples. The pPHT01 and pPHT14 plasmids each contain two parts of our system (Figure 1B), the evolved *lsr* promoters (EP01rec or EP14rec) and the pBAD controlled *lsrR* repressor subcircuit. The third component (LsrK background) is enabled by pSkunk-*lsrK* (Figure 1B), which maintains an elevated LsrK kinase level that ensures uptake and phosphorylation of AI-2, allowing LsrR to release the *lsr* promoter *via* derepression. Our decision to incorporate the *pBAD* promoter was based on its tight regulation and facile modulation *via* arabinose addition.[69] When envisioning future applications, this feature retains homologous QS (hQS) regulation for *in vivo* purposes such as "smart" probiotic use in drug-delivery and diagnosis applications. That is, the extra control is enabled by simple carbohydrate (arabinose) addition. Importantly, the third component, LsrK, maintains circuit sensitivity to the prevailing AI-2 level. Here, the hybrid *tac* promoter was used because it has a high background level of basal LsrK so that the prevailing AI-2 level is rapidly converted into viable genetic signal.[34,67,68] While not described thus far, our *E. coli* host strains were also engineered to achieve better control of protein expression levels. Notably, because our focus is on the homologous QS circuitry and the *lsr* promoter of *E. coli*, which is a component of native *E. coli* quorum sensing (Figure 1A), our host cell has additional mutations (*e.g.*, Δ*ptsH*) that ensure our host functions with advanced sensitivity to AI-2 and for a variety of environmental niches.[70] The *luxS* gene was also deleted. LuxS is a *S*-ribosylhomocysteinase that catalyzes the last committed step in the biosynthetic pathway of AI-2, which is the autoinducer in our system. Thus, the engineered cells

https://dx.doi.org/10.1021/acssynbio.0c00179
ACS Synth. Biol. 2020, 9, 2692−2702

respond to the prevailing AI-2 level, rather than contribute to it. Our tested systems include *E. coli* Nissle 1917 (a commensal host) and *E. coli* PH04 (see Supplemental Table S1). We previously discovered that deletion of *ptsH* enables homologous AI-2 QS in the presence of glucose.[70] That is, *ptsH* encodes HPr, which is involved in the central phosphotransferase system (PTS) for sugar uptake; we found HPr forms dimers with LsrK, inhibiting its activity and altering native QS. The extent of inhibition is dependent on the phosphorylation state of HPr, which varies depending on whether glucose is being transported into the cell. Additionally, Lsr is directly regulated by CRP owing to the CRP binding site located in the *lsrR*/*lsrA* intergenic region.[46,47] These functions all serve to diminish QS signaling among *E. coli* and other genera[45] in the presence of glucose. Manipulation or removal of these controls in the host cells enables QS modulation in the presence of glucose and a variety of other conditions.[48,57,70,71] In Supplemental Figure S1, we found no growth impairment in PH04 due to AI-2 and arabinose addition.

Ara-Mediated QS Repression *via* LsrR. In our semisynthetic QS regulator, we make use of the native QS repressor, LsrR. In Figure 2, we measured the level of GFP expressed *via* the EP01rec and EP14rec promoters and repressed by the araC-induced overexpression of LsrR. *E. coli* PH04 cells (Δ*luxS* Δ*ptsH*) carrying hQSRC01 or hQSRC14 were either grown in LB media to OD_{600} ∼ 0.2 and then supplemented with arabinose at 0.002% or were grown from inoculation (*e.g.*, OD_{600} ∼ 0.02) in the presence of 0.02% and 0.2% arabinose. We measured GFP fluorescence *via* FACS at OD_{600} ∼ 0.2, and after 2 and 4 h of additional cell growth. These experiments enable elucidation of both the extent of repression and its transient nature. In all cases the addition of more than 0.02% arabinose resulted in a tightly repressed state and this was maintained throughout. Interestingly, in the experiments where arabinose was added at OD_{600} ∼ 0.2, even 0.002% arabinose prevented the subsequent induction of GFP (the levels at OD_{600} ∼ 0.2 were maintained at 2 and 4 h). We further note that the absence of arabinose enabled the native-like (*e.g.*, leaky) expression of GFP previously observed in EP01rec and EP14rec.[57] The PH04 strain used to perform the experiment is not an AI-2 producer (Δ*luxS*), and AI-2 was not added to these cultures. We note that the EP01rec promoter was previously shown to exhibit more leaky expression than the EP14rec promoter,[57] which is likely the cause for relatively higher GFP levels shown here.

Dual Input Control of Homologous QS Signaling. Having demonstrated that even low levels of arabinose provide for repression of the genetic circuit, we wanted to test the release of this repression by the addition of the native QS signal molecule, AI-2. In this way, the genetic circuit would exhibit low or no expression of the encoded target gene unless AI-2 was present. Experiments were performed combining arabinose (repressor) and AI-2 (inducer). For this, cultures were grown in LB media prepared with 0, 0.005 and 0.01% arabinose, and then at $OD_{600\ nm}$ ∼ 0.2, different concentrations of AI-2 (0, 40, or 80 μM AI-2) were added to cell cultures. On the basis of our previous results (Figure 2), we determined 0.005 and 0.01% arabinose would correspond to a minimal and maximal repression condition, over which we could test AI-2 mediated derepression. That is, with higher levels of arabinose (*e.g.*, 0.02%, Figure 2), we suspect that subsequent AI-2 addition would have minimal impact. GFP fluorescence was measured at $OD_{600\ nm}$ ∼ 0.2, which is the induction point, and after 2, 4, 6, and 9 h. In Figure 3A, we found expression levels in both systems (hQSRC01 and hQSRC14) were reduced by

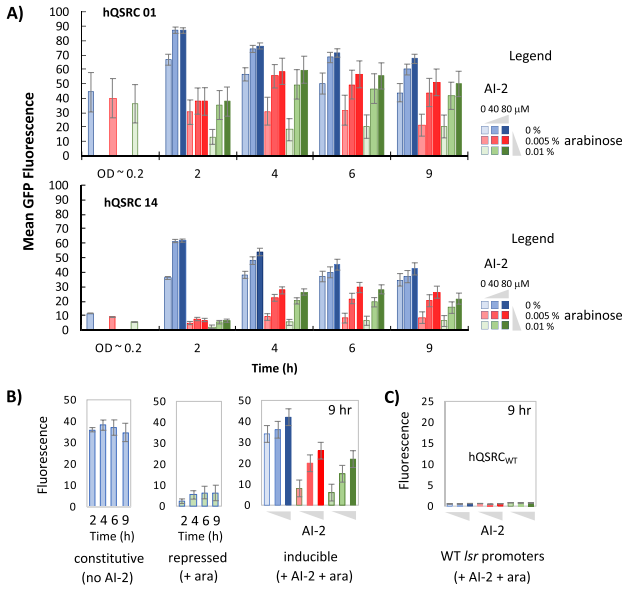

Figure 3. Transcriptional regulation of hQSRC01 and hQSRC14 in the presence or absence of arabinose (repressor) and/or AI-2 (inducer). PH04 cells carry hQSRC01 or hQSRC14 system expressing GFP. (A) Panels represent different time points during cell growth (2, 4, 6, and 9 h); samples were collected for measurement of GFP fluorescence. Bar color (blue, red, or green) indicates whether arabinose was added; color intensity (faded to strong) indicates the level of AI-2 supplemented, as indicated. (B) Data from the hQSRC14 system in A are recast into the three different modes of operation: (i) constitutive, (ii) repressed by arabinose addition, and (iii) induced by AI-2 either with or without arabinose. (C) Full time course of data from $hQSRC_{WT}$, which is identical to hQSRC but with the native *lsr* promoter. Extra repression is clearly visible. Data are plotted as means ± standard deviations of technical triplicates of duplicate runs.

at least ∼50% in the presence of 0.005 and 0.01% arabinose, when compared to expression in the absence of arabinose, as expected. Then, both hQSRC01 and hQSRC14 were switched ON in the presence of 40 or 80 μM AI-2 (inducer), even in the presence of 0.005 or 0.01% arabinose. 80 μM AI-2 consistently resulted in higher activation than 40 μM AI-2, consistent with previous results showing that the *lsr* promoter is tunable over a range of AI-2 concentrations.[72] hQSRC01 showed higher expression levels in comparison to hQSRC14 (Figure 3A), but as noted earlier, this is likely due to more constitutive expression in the absence of repressor or inducer (see OD_{600} ∼ 0.2 used as controls). In both systems, arabinose-mediated repression was sustained or derepressed (by AI-2 addition) and the resulting expression levels were maintained while the cells grew from 0.2 to the final OD (∼OD_{600} = 4).

Our results suggest that the dual input hQSRC system, which makes use of an added metabolizable carbohydrate and the homologous AI-2 QS signal could be "operated" in three different modes: (1) there is a well-defined constitutive expression mode when neither the arabinose nor AI-2 are present (*e.g.*, no repression and no induction), (2) a controllable repression mode in which tight LsrR repression is rapidly induced by the addition of arabinose, and (3) a repression/induction mode *via* native AI-2 signaling with levels

https://dx.doi.org/10.1021/acssynbio.0c00179
ACS Synth. Biol. 2020, 9, 2692−2702

that are tuned by the prevailing AI-2 level. Figure 3B shows the hQSRC14 operated in each of these three modes. Both hQSRC01 and hQSRC14 made use of evolved promoter regions of the native *lsr* promoter which had advantageous characteristics (*e.g.*, higher expression and more amplification relative to the wild type). For instance, Figure 3C shows that in an identical system with the native *lsr* promoter driving GFP expression rather than the evolved promoters (called $hQSRC_{WT}$), GFP expression levels remain low even with AI-2 addition.

In Supplemental Tables S3 and S4 and Supplemental Note S1, we describe a simple ODE-based mathematical model that enables dynamic simulation of gene expression using these circuits. In particular, the model equations employ standard forms of repression and activation (as mediated by a single transcriptional regulator). The model was developed to accommodate arabinose-induced LsrR, as well as LsrR and AI-2-mediated regulation of *lsr* promoter activity. Its utility is in its discriminatory ability to tease out the relative amplification (fold change) that is obtained by having the extra repression enabled by overexpressed LsrR. That is, a central purpose for designing this system was to first provide low background expression but then develop autoinduced amplification that responds strongly to AI-2. This is an alternative motivation to that of our previous work in which we sought only amplification of *lsr*-mediated expression by using a T7 amplification scheme.[51,73] We simulated the experiment carried out in Figure 3A (hQSRC01) using the model, adjusting the unknown model parameters (*e.g.*, repressor binding, K_{LsrR}, transcription rate, β_{GFP}) so the model and experimental results were in reasonable agreement. In Supplemental Figures S2 and S3, cell growth and expression results for all levels of arabinose and AI-2 are depicted. For simplicity, Figure 4A shows the strong agreement between the model and the data for the 0.01% arabinose cases of hQSRC01. This agreement suggests that the general model formalism and constants are reasonable. We subsequently altered the GFP transcription rate constant, β_{GFP}, to simulate the hQSRC14 system, anticipating that this should be the only altered parameter between the two systems (the host and remaining genetic control components are identical). To do this, we simply halved the rate constant based on our previous data showing mRNA and the expression levels of two target genes[57] using the EP14rec promoter were at about half the levels of the EP01rec promoter. The simulated GFP levels were again within experimental error. Again, this result confirms that the genetic circuit as modeled by a set of ordinary differential equations (ODE) reasonably reflects the level of gene expression from this dual-input controller. We have quantified the differences between the model and experiments by including Supplemental Figure S4, which depicts each data point with its corresponding simulated value. In general, we found the model deviation was within 20−40% of the experimental values for both cases and throughout all times.

Engineered Probiotic Bacteria Secreting Active Recombinant Human GM-CSF *via* hQSRC System. Armed with a predictive model, especially one that characterizes the extra control that is enabled by arabinose controlled LsrR-repression and AI-2 derepression, one can use this formalism to design expression characteristics for therapeutic proteins, ultimately enabling a base model for "smart probiotic" delivery systems for complex *in vivo* environments.

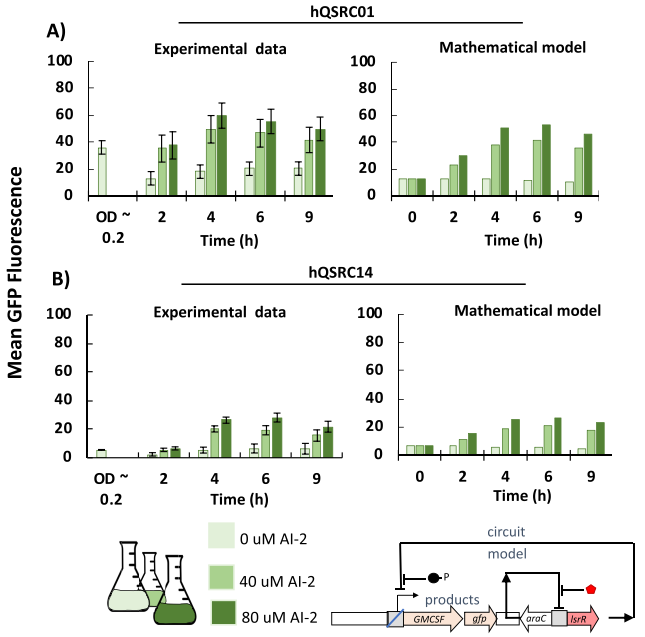

Figure 4. Comparison of experimental data to model simulations. (A) hQSRC01 data (left) were used to ensure reasonable agreement with model (right). (B) On the basis of previous measurements of promoter strength,[57] one model parameter, β_{GFP} (Supplemental Table S4), was adjusted to predict behavior of hQSRC14. Model equations, parameters, and assumptions along with other simulations are provided in Supplemental Tables S3, S4 and Supplemental Note S1.

E. coli Nissle 1917 (EcN) is a commensal *E. coli* strain that has been widely used in many studies involving probiotics and the production of biotherapeutics.[5,74−77] We engineered EcN to create *E. coli* PH08 which is a *luxS* and *ptsH* double knockout of the isogenic parent. In this way, alterations of the genetic background used to construct PH04 with results from Figure 4 were maintained. Naturally, the rest of the genetic backgrounds for the two strains were different. Next, pPHT01 and pPHT14 were modified to express a granulocyte macrophage colony stimulating factor (GM-CSF), a model gastrointestinal (GI) tract therapeutic[7,73] Here, we express a chimeric protein consisting of a secretion mediator, YebF, an enterokinase cleavage site, and a C-terminal hexahistidine tag for purification *via* immobilized metal ion affinity chromatography (IMAC). The YebF-EK-rhGM-CSF-His6 fusion construct (rhGM-CSF chimera) was placed in front of the *gfpmut2* gene, both under EP01rec or EP14rec control, thus creating pPHT01-rhGM-CSF chimera and pPHT14-rhGM-CSF chimera, respectively.

The *E. coli* PH08 strain expressing rhGM-CSF chimera *via* hQSRC01 or hQSRC14 system were cultivated in various conditions including (or not) the repressor signal (arabinose) or inducer signal (AI-2). Subsequently, we expected GM-CSF would be expressed and secreted into the extracellular media at various levels according to the signaling conditions. After 4 h of induction or repression, supernatants from each culture were collected and precipitated using a TCA protocol as described in Materials and Methods followed by Western blot. In Figure 5A, the rhGM-CSF chimera was detected in the positive control (denoted "C"), where the pAES40 plasmid was used to express the chimeric protein under the *tac* promoter *via* IPTG addition. For hQSRC01, rhGM-CSF chimera expression was significantly lower due to the added presence of 0.01%

https://dx.doi.org/10.1021/acssynbio.0c00179
ACS Synth. Biol. 2020, 9, 2692−2702

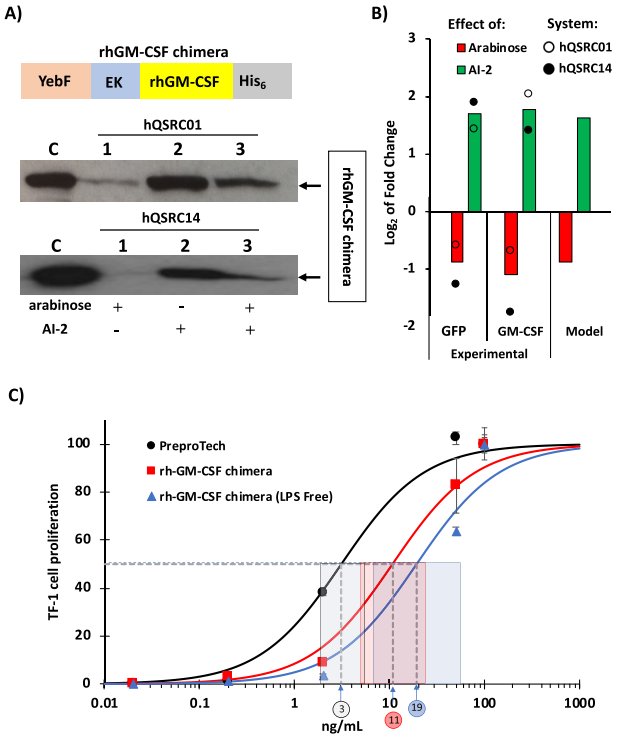

Figure 5. Dual-input controlled expression of rhGM-CSF. (A) Recombinant human GM-CSF chimera (rhGM-CSF chimera) expression and secretion in *E. coli* Nissle Δ*lux*S Δ*ptsH* strain (PH08). PH08 cells were grown in LB media and supplemented with 0.01% arabinose and/or 40 μM AI-2. The rhGM-CSF chimera expressed extracellularly was analyzed using Western blots. Samples from different growth conditions were precipitated using a TCA protocol. Lanes indicated were (1) A positive control (pAES40-GM-CSF induced *via* IPTG), (2) 0.01% arabinose, (3) 40 μM AI-2, and (4) 40 μM AI-2 plus 0.01% arabinose. (B) AI-2 and arabinose-mediated fold change in expression of GFP and rhGM-CSF chimera after 4 h growth in the presence of 0.01% arabinose and after AI-2 addition (40 μM). Here, the effect of arabinose was evaluated from Western data in A, where the intensity of blots from Lane 3 data (with AI-2 and arabinose) were divided by Lane 2 (with AI-2 and without arabinose). AI-2 mediated fold change is shown as expression levels with 0.01% arabinose and 40 μM AI-2 addition relative to the same experimental setup without AI-2 (Lane 3 divided by Lane 1 in (A)). Fold changes in GFP expression were determined from Figure 3. The open and closed circles represent fold changes for either hQSRC01 or hQSRC14, as indicated. The bars represent the average fold changes of both systems. Note that the model predicts the same fold changes for both hQSRC01 and hQSRC14. (C) Purified and depyrogenated (LPS free) rhGM-CSF chimera expressed by PH08 strain was bioactive as noted by proliferation of TF-1 cells. Activity was also compared to the commercially available hGM-CSF (PeproTech). Calculated EC50 values with 95% confidence bounds are shown for each sample.

arabinose (repressor signal, Lane 1). We note that the rhGM-CSF chimera was observed in both conditions in which AI-2 was added to the culture, 40 μM AI-2 and 40 μM AI-2 plus 0.01% arabinose (Lanes 2 and 3). Importantly, in the condition that both inducer and repressor were added (Lane 3), rhGM-CSF chimera levels were higher with AI-2 only (Figure 5A, Lane 2). Analogously, the hQSRC14 system showed similar protein expression profiles to hQSRC01; however, since EP14rec is a weaker promoter compared to EP01rec, protein expression levels were somewhat lower in comparison. Both systems exhibited the repressible and inducible phenotype shown dynamically and at more conditions for the GFP experiments. In Figure 5B, we compared repression and induction of GFP (Figure 3) to the repression and induction of rhGM-CSF chimera estimated from the gel images (Figure 5A, gel image quantification illustrated in Supplemental Figure S5). We also show the results predicted by the mathematical model. That is, we previously demonstrated that the model was in agreement with the GFP fluorescence data (Figure 4), and here we used the model to predict outcomes using rhGM-CSF chimera as a product. We compare conditions with or without arabinose and AI-2 as a means to normalize the data. While the model can provide a molar concentration of rhGM-CSF chimera, it is the fold-change and tunability that we are most interested in capturing. By describing fold change, the stoichiometric constants that convert transcript level to concentration of protein are factored out. Without altering transcription rate constants, the 4 h time points after AI-2 addition from the model were used to compare to the rhGM-CSF chimera expression experiments (Figure 5B). Here, the effect of arabinose was evaluated from Western blot data in Figure 5A, where the intensity of bands from Lane 3 data were divided by Lane 2. The effect of AI-2 is shown as the expression level with 0.01% arabinose and 40 μM AI-2 addition relative to the same experimental setup without AI-2 (Lane 3 divided by Lane 1 in (Figure 5A). Note that the model predicts the same fold changes for both hQSRC01 and hQSRC14 since the only difference in the model between the two systems was the transcription rate constant for the gene-of-interest, which is factored out when determining fold change. Experimentally, AI-2 or arabinose mediated fold changes were similar between the two systems for both the GFP and rhGM-CSF chimera expression experiments (dots represent average results for the individual systems, while the bars represent averages of the two systems, Figure 5B). The expression model correlated extremely well with the repression and subsequent AI-2-mediated derepression, illustrating that for GM-CSF, a secreted protein of mammalian origin the model was still viable. This suggests that the model generated for hQSRC system may have potential for future designs and more importantly, it corroborates the mechanistic relationships between the promoter and repressor designs in the model equations. Thus, the expression and secretion of human GM-CSF (*i.e.*, rhGM-CSF chimera) using an engineered commensal *E. coli* strain (PH08) may serve as a step toward a viable "smart" probiotic delivery system. While not shown here, the extra benefit enabled by the tight arabinose-mediated repression is that potentially cell toxins (*e.g.*, cancer therapeutics) could be delivered in a more spatially or temporally controlled manner. Our data also suggest the expression of a protein or other molecule could potentially be stopped by the exogenous (or otherwise) addition of arabinose. That is, the rhGM-CSF chimera could be constitutively expressed and then stopped. There might be advantages to all three modes of expression and control (i.e., switched from one mode to the other).

To ascertain whether the rhGM-CSF chimera expressed and secreted was biologically active, supernatants collected after 4 h of protein expression were passed through a Ni^{2+}-Sepharose column, purified, and evaluated using a human TF-1 cell line, wherein proliferation is stimulated by rhGM-CSF.[78] Since LPS interacts directly with a TLR4/MD-2 complex on hemato-poietic progenitor cells,[79] we also depyrogenated the purified chimera by incubating with polymyxin B sulfate to remove

https://dx.doi.org/10.1021/acssynbio.0c00179
ACS Synth. Biol. 2020, 9, 2692−2702

possible LPS contamination from the host *E. coli* cells. In Figure 5C, TF-1 cell proliferation was higher for the GM-CSF purchased from PeproTech than the rhGM-CSF chimera expressed *via* hQSRC01 in PH08 host cells at most concentrations tested. However, the *E. coli* expressed protein was also quite active; differences could be due to many factors including potential effects from *yebF* fusion with membrane translocation and purification tags. We also note that the samples treated with polymyxin B showed further decreased TF-1 cell proliferation when compared with the other samples (Figure 5C), indicating a possible activation effect by LPS. To quantify differences in activity, we fit each data set to a logistic curve and determined the best fit value for EC50, or the concentration of sample that resulted in 50% of the maximum activity. The EC50 values were 3, 11, and 19 ng/μL for the purchased GM-CSF, expressed rhGM-CSF chimera, and LPS free rhGM-CSF chimera, respectively. Perhaps more importantly, a 250 mL culture of PH08 cells carrying the hQSRC01 GM-CSF expression system yielded ~100 μg/mL of active YebF-EK-hGM-CSF-His6 fusion, which is appreciable.

CONCLUSIONS

We created a semisynthetic QS regulator, the *E. coli* homologous quorum sensing regulatory circuit (hQSRC) that enables both external and endogenous control of gene expression based on native AI-2 signaling. This was built upon our previous directed evolution efforts of the *lsr* promoters;[57] key features of the new system are due to the rewiring and adjusting of the AI-2 QS regulatory components, LsrK and LsrR. Here, we enabled tighter than native repression by the addition of the heterologous arabinose repressor/actuator system and more sensitive AI-2 mediated activation by the incorporation of additional levels of LsrK.[68] To transition this system toward *in vivo* application, we added these constructs to *luxS* and *ptsH* deletion mutants enabling their function in the presence of glucose and precluding extraneous signaling by AI-2 synthesis. Further, we built a mathematical model that can be used to estimate protein production based on both the native and external cues. We believe the novelty and value of this system is that it builds tunable control onto the homologous (AI-2) signaling processes native to *E. coli* and many other bacteria, both Gram positive and Gram negative, as well as by the addition of a simple digestible sugar. Its tight repression until AI-2 accumulates for derepression is attractive for industrial biotechnological settings, and its two-cue processing logic should enable robust use in complex environments.

ASSOCIATED CONTENT

Supporting Information

The Supporting Information is available free of charge at https://pubs.acs.org/doi/10.1021/acssynbio.0c00179.

Cell growth curves (Figure S1), quantification of gel images (Figure S5), strains, plasmids, and primers used in this study (Tables S1, S2), and details describing mathematical model (Tables S3, S4, Note S1, Figures S2–S4) (PDF)

AUTHOR INFORMATION

Corresponding Author

William E. Bentley − *Institute for Bioscience and Biotechnology Research, College Park, Maryland 20742, United States; Fischell Department of Bioengineering and Robert E. Fischell Institute for Biomedical Devices, University of Maryland, College Park, Maryland 20742, United States;* orcid.org/0000-0002-4855-7866; Phone: +1-301-405-4321; Email: bentley@umd.edu; Fax: +1-301-405-9953

Authors

Pricila Hauk − *Institute for Bioscience and Biotechnology Research, College Park, Maryland 20742, United States; Fischell Department of Bioengineering, University of Maryland, College Park, Maryland 20742, United States*

Kristina Stephens − *Institute for Bioscience and Biotechnology Research, College Park, Maryland 20742, United States; Fischell Department of Bioengineering and Robert E. Fischell Institute for Biomedical Devices, University of Maryland, College Park, Maryland 20742, United States*

Chelsea Virgile − *Institute for Bioscience and Biotechnology Research, College Park, Maryland 20742, United States; Fischell Department of Bioengineering, University of Maryland, College Park, Maryland 20742, United States*

Eric VanArsdale − *Institute for Bioscience and Biotechnology Research, College Park, Maryland 20742, United States; Fischell Department of Bioengineering and Robert E. Fischell Institute for Biomedical Devices, University of Maryland, College Park, Maryland 20742, United States*

Alex Eli Pottash − *Fischell Department of Bioengineering, University of Maryland, College Park, Maryland 20742, United States*

John S. Schardt − *Fischell Department of Bioengineering, University of Maryland, College Park, Maryland 20742, United States*

Steven M. Jay − *Fischell Department of Bioengineering, University of Maryland, College Park, Maryland 20742, United States;* orcid.org/0000-0002-3827-5988

Herman O. Sintim − *Department of Chemistry and Institute for Drug Discovery, Purdue University, West Lafayette, Indiana 47907, United States*

Complete contact information is available at: https://pubs.acs.org/10.1021/acssynbio.0c00179

Notes

The authors declare no competing financial interest.

ACKNOWLEDGMENTS

Defense Threat Reduction Agency (DTRA) [HDTRA 1-13-1-00037, HDTRA1-19-0021]; US National Science Foundation [CBET# 1805274, DMREF#1435957]; and the National Institutes of Health [R21EB024102].

REFERENCES

(1) Kang, M., Lu, Y., Chen, S., and Tian, F. (2018) Harnessing the power of an expanded genetic code toward next-generation biopharmaceuticals. *Curr. Opin. Chem. Biol. 46*, 123−129.

(2) Forbes, N. S. (2010) Engineering the perfect (bacterial) cancer therapy. *Nat. Rev. Cancer 10*, 785−794.

(3) Hwang, I. Y., Koh, E., Wong, A., March, J. C., Bentley, W. E., Lee, Y. S., and Chang, M. W. (2017) Engineered probiotic Escherichia coli can eliminate and prevent Pseudomonas aeruginosa gut infection in animal models. *Nat. Commun. 8*, 15028.

(4) Panteli, J. T., Van Dessel, N., and Forbes, N. S. (2020) Detection of tumors with fluoromarker-releasing bacteria. *Int. J. Cancer 146*, 137−149.

(5) Hwang, I. Y., and Chang, M. W. (2020) Engineering commensal bacteria to rewire host-microbiome interactions. *Curr. Opin. Biotechnol. 62*, 116−122.

(6) Hwang, I. Y., Tan, M. H., Koh, E., Ho, C. L., Poh, C. L., and Chang, M. W. (2014) Reprogramming microbes to be pathogen-seeking killers. *ACS Synth. Biol. 3*, 228−237.
(7) McKay, R., Ghodasra, M., Schardt, J., Quan, D., Pottash, A. E., Shang, W., Jay, S. M., Payne, G. F., Chang, M. W., March, J. C., and Bentley, W. E. (2018) A platform of genetically engineered bacteria as vehicles for localized delivery of therapeutics: Toward applications for Crohn's disease. *Bioeng Transl Med. 3*, 209−221.
(8) Geldart, K. G., Kommineni, S., Forbes, M., Hayward, M., Dunny, G. M., Salzman, N. H., and Kaznessis, Y. N. (2018) Engineered E. coli Nissle 1917 for the reduction of vancomycin-resistant Enterococcus in the intestinal tract. *Bioeng Transl Med. 3*, 197−208.
(9) Geldart, K., Forkus, B., McChesney, E., McCue, M., and Kaznessis, Y. N. (2016) pMPES: A Modular Peptide Expression System for the Delivery of Antimicrobial Peptides to the Site of Gastrointestinal Infections Using Probiotics. *Pharmaceuticals 9*, 60.
(10) Van Dessel, N., Swofford, C. A., and Forbes, N. S. (2015) Potent and tumor specific: arming bacteria with therapeutic proteins. *Ther. Delivery 6*, 385−399.
(11) Duan, F. F., Liu, J. H., and March, J. C. (2015) Engineered commensal bacteria reprogram intestinal cells into glucose-responsive insulin-secreting cells for the treatment of diabetes. *Diabetes 64*, 1794−1803.
(12) Hwang, I. Y., Lee, H. L., Huang, J. G., Lim, Y. Y., Yew, W. S., Lee, Y. S., and Chang, M. W. (2018) Engineering microbes for targeted strikes against human pathogens. *Cell. Mol. Life Sci. 75*, 2719−2733.
(13) Ou, B., Jiang, B., Jin, D., Yang, Y., Zhang, M., Zhang, D., Zhao, H., Xu, M., Song, H., Wu, W., Chen, M., Lu, T., Huang, J., Seo, H., Garcia, C., Zheng, W., Guo, W., Lu, Y., Jiang, Y., Yang, S., Kaushik, R. S., Li, X., Zhang, W., and Zhu, G. (2020) Engineered Recombinant Escherichia coli Probiotic Strains Integrated with F4 and F18 Fimbriae Cluster Genes in the Chromosome and Their Assessment of Immunogenic Efficacy in Vivo. *ACS Synth. Biol. 9*, 412−426.
(14) Rottinghaus, A. G., Amrofell, M. B., and Moon, T. S. (2020) Biosensing in Smart Engineered Probiotics. *Biotechnol. J.*, No. e1900319.
(15) El Hage, R., Hernandez-Sanabria, E., and Van de Wiele, T. (2017) Emerging Trends in "Smart Probiotics": Functional Consideration for the Development of Novel Health and Industrial Applications. *Front. Microbiol. 8*, 1889.
(16) Landry, B. P., and Tabor, J. J. (2017) Engineering Diagnostic and Therapeutic Gut Bacteria. *Microbiol. Spectr.*, DOI: 10.1128/microbiolspec.BAD-0020-2017.
(17) Swofford, C. A., Van Dessel, N., and Forbes, N. S. (2015) Quorum-sensing Salmonella selectively trigger protein expression within tumors. *Proc. Natl. Acad. Sci. U. S. A. 112*, 3457−3462.
(18) Duan, F., and March, J. C. (2010) Engineered bacterial communication prevents Vibrio cholerae virulence in an infant mouse model. *Proc. Natl. Acad. Sci. U. S. A. 107*, 11260−11264.
(19) Mimee, M., Tucker, A. C., Voigt, C. A., and Lu, T. K. (2016) Programming a Human Commensal Bacterium, Bacteroides thetaiotaomicron, to Sense and Respond to Stimuli in the Murine Gut Microbiota. *Cell Syst 2*, 214.
(20) Mao, N., Cubillos-Ruiz, A., Cameron, D. E., and Collins, J. J. (2018) Probiotic strains detect and suppress cholera in mice. *Sci. Transl. Med. 10*, No. eaao2586.
(21) Virgile, C., Hauk, P., Wu, H. C., Shang, W., Tsao, C. Y., Payne, G. F., and Bentley, W. E. (2018) Engineering bacterial motility towards hydrogen-peroxide. *PLoS One 13*, No. e0196999.
(22) Shang, W., Tsao, C. Y., Luo, X., Teodoro, M., McKay, R., Quan, D. N., Wu, H. C., Payne, G. F., and Bentley, W. E. (2017) A simple and reusable bilayer membrane-based microfluidic device for the study of gradient-mediated bacterial behaviors. *Biomicrofluidics 11*, 044114.
(23) Terrell, J. L., Wu, H. C., Tsao, C. Y., Barber, N. B., Servinsky, M. D., Payne, G. F., and Bentley, W. E. (2015) Nano-guided cell networks as conveyors of molecular communication. *Nat. Commun. 6*, 8500.
(24) Panteli, J. T., and Forbes, N. S. (2016) Engineered bacteria detect spatial profiles in glucose concentration within solid tumor cell masses. *Biotechnol. Bioeng. 113*, 2474−2484.
(25) Forbes, N. S., Coffin, R. S., Deng, L., Evgin, L., Fiering, S., Giacalone, M., Gravekamp, C., Gulley, J. L., Gunn, H., Hoffman, R. M., Kaur, B., Liu, K., Lyerly, H. K., Marciscano, A. E., Moradian, E., Ruppel, S., Saltzman, D. A., Tattersall, P. J., Thorne, S., Vile, R. G., Zhang, H. H., Zhou, S., and McFadden, G. (2018) White paper on microbial anti-cancer therapy and prevention. *J. Immunother. Cancer 6*, 78.
(26) Khalil, A. S., and Collins, J. J. (2010) Synthetic biology: applications come of age. *Nat. Rev. Genet. 11*, 367−379.
(27) Hong, S. H., Hegde, M., Kim, J., Wang, X., Jayaraman, A., and Wood, T. K. (2012) Synthetic quorum-sensing circuit to control consortial biofilm formation and dispersal in a microfluidic device. *Nat. Commun. 3*, 613.
(28) Hol, F. J., and Dekker, C. (2014) Zooming in to see the bigger picture: microfluidic and nanofabrication tools to study bacteria. *Science 346*, 1251821.
(29) Balagadde, F. K., You, L., Hansen, C. L., Arnold, F. H., and Quake, S. R. (2005) Long-term monitoring of bacteria undergoing programmed population control in a microchemostat. *Science 309*, 137−140.
(30) Fernandes, R., Luo, X., Tsao, C. Y., Payne, G. F., Ghodssi, R., Rubloff, G. W., and Bentley, W. E. (2010) Biological nanofactories facilitate spatially selective capture and manipulation of quorum sensing bacteria in a bioMEMS device. *Lab Chip 10*, 1128−1134.
(31) Luo, X., Tsao, C. Y., Wu, H. C., Quan, D. N., Payne, G. F., Rubloff, G. W., and Bentley, W. E. (2015) Distal modulation of bacterial cell-cell signalling in a synthetic ecosystem using partitioned microfluidics. *Lab Chip 15*, 1842−1851.
(32) Ueda, H., Stephens, K., Trivisa, K., and Bentley, W. E. (2019) Bacteria Floc, but Do They Flock? Insights from Population Interaction Models of Quorum Sensing. *mBio 10*, No. e00972-19.
(33) Ravichandar, J. D., Bower, A. G., Julius, A. A., and Collins, C. H. (2017) Transcriptional control of motility enables directional movement of Escherichia coli in a signal gradient. *Sci. Rep. 7*, 8959.
(34) Zargar, A., Quan, D. N., Emamian, M., Tsao, C. Y., Wu, H. C., Virgile, C. R., and Bentley, W. E. (2015) Rational design of 'controller cells' to manipulate protein and phenotype expression. *Metab. Eng. 30*, 61−68.
(35) Marguet, P., Tanouchi, Y., Spitz, E., Smith, C., and You, L. (2010) Oscillations by minimal bacterial suicide circuits reveal hidden facets of host-circuit physiology. *PLoS One 5*, No. e11909.
(36) Ward, J. P., King, J. R., Koerber, A. J., Williams, P., Croft, J. M., and Sockett, R. E. (2001) Mathematical modelling of quorum sensing in bacteria. *IMA J. Math Appl. Med. Biol. 18*, 263−292.
(37) Viretta, A. U., and Fussenegger, M. (2004) Modeling the quorum sensing regulatory network of human-pathogenic Pseudomonas aeruginosa. *Biotechnol. Prog. 20*, 670−678.
(38) Duan, F., and March, J. C. (2008) Interrupting Vibrio cholerae infection of human epithelial cells with engineered commensal bacterial signaling. *Biotechnol. Bioeng. 101*, 128−134.
(39) Saeidi, N., Wong, C. K., Lo, T. M., Nguyen, H. X., Ling, H., Leong, S. S., Poh, C. L., and Chang, M. W. (2011) Engineering microbes to sense and eradicate Pseudomonas aeruginosa, a human pathogen. *Mol. Syst. Biol. 7*, 521.
(40) Gupta, A., Reizman, I. M., Reisch, C. R., and Prather, K. L. (2017) Dynamic regulation of metabolic flux in engineered bacteria using a pathway-independent quorum-sensing circuit. *Nat. Biotechnol. 35*, 273−279.
(41) Tamsir, A., Tabor, J. J., and Voigt, C. A. (2011) Robust multicellular computing using genetically encoded NOR gates and chemical 'wires'. *Nature 469*, 212−215.
(42) Shong, J., and Collins, C. H. (2014) Quorum sensing-modulated AND-gate promoters control gene expression in response to a combination of endogenous and exogenous signals. *ACS Synth. Biol. 3*, 238−246.

(43) Hu, Y., Yang, Y., Katz, E., and Song, H. (2015) Programming the quorum sensing-based AND gate in Shewanella oneidensis for logic gated-microbial fuel cells. *Chem. Commun. 51*, 4184−4187.
(44) Zargar, A., Quan, D. N., Carter, K. K., Guo, M., Sintim, H. O., Payne, G. F., and Bentley, W. E. (2015) Bacterial secretions of nonpathogenic Escherichia coli elicit inflammatory pathways: a closer investigation of interkingdom signaling. *mBio 6*, No. e00025.
(45) Quan, D. N., and Bentley, W. E. (2012) Gene network homology in prokaryotes using a similarity search approach: queries of quorum sensing signal transduction. *PLoS Comput. Biol. 8*, No. e1002637.
(46) Wang, L., Li, J., March, J. C., Valdes, J. J., and Bentley, W. E. (2005) luxS-dependent gene regulation in Escherichia coli K-12 revealed by genomic expression profiling. *J. Bacteriol. 187*, 8350−8360.
(47) Wang, L., Hashimoto, Y., Tsao, C. Y., Valdes, J. J., and Bentley, W. E. (2005) Cyclic AMP (cAMP) and cAMP receptor protein influence both synthesis and uptake of extracellular autoinducer 2 in Escherichia coli. *J. Bacteriol. 187*, 2066−2076.
(48) Xavier, K. B., and Bassler, B. L. (2005) Regulation of uptake and processing of the quorum-sensing autoinducer AI-2 in Escherichia coli. *J. Bacteriol. 187*, 238−248.
(49) Xavier, K. B., Miller, S. T., Lu, W., Kim, J. H., Rabinowitz, J., Pelczer, I., Semmelhack, M. F., and Bassler, B. L. (2007) Phosphorylation and processing of the quorum-sensing molecule autoinducer-2 in enteric bacteria. *ACS Chem. Biol. 2*, 128−136.
(50) Tsao, C. Y., Wang, L., Hashimoto, Y., Yi, H., March, J. C., DeLisa, M. P., Wood, T. K., Valdes, J. J., and Bentley, W. E. (2011) LuxS coexpression enhances yields of recombinant proteins in Escherichia coli in part through posttranscriptional control of GroEL. *Appl. Environ. Microbiol. 77*, 2141−2152.
(51) Tsao, C. Y., Hooshangi, S., Wu, H. C., Valdes, J. J., and Bentley, W. E. (2010) Autonomous induction of recombinant proteins by minimally rewiring native quorum sensing regulon of *E. coli*. *Metab. Eng. 12*, 291−297.
(52) Wu, H. C., Tsao, C. Y., Quan, D. N., Cheng, Y., Servinsky, M. D., Carter, K. K., Jee, K. J., Terrell, J. L., Zargar, A., Rubloff, G. W., Payne, G. F., Valdes, J. J., and Bentley, W. E. (2013) Autonomous bacterial localization and gene expression based on nearby cell receptor density. *Mol. Syst. Biol. 9*, 636.
(53) Quan, D. N., Tsao, C. Y., Wu, H. C., and Bentley, W. E. (2016) Quorum Sensing Desynchronization Leads to Bimodality and Patterned Behaviors. *PLoS Comput. Biol. 12*, No. e1004781.
(54) Li, J., Wang, L., Hashimoto, Y., Tsao, C. Y., Wood, T. K., Valdes, J. J., Zafiriou, E., and Bentley, W. E. (2006) A stochastic model of Escherichia coli AI-2 quorum signal circuit reveals alternative synthesis pathways. *Mol. Syst. Biol. 2*, 67.
(55) Hooshangi, S., and Bentley, W. E. (2011) LsrR quorum sensing "switch" is revealed by a bottom-up approach. *PLoS Comput. Biol. 7*, No. e1002172.
(56) Adams, B. L., Carter, K. K., Guo, M., Wu, H. C., Tsao, C. Y., Sintim, H. O., Valdes, J. J., and Bentley, W. E. (2014) Evolved Quorum sensing regulator, LsrR, for altered switching functions. *ACS Synth. Biol. 3*, 210−219.
(57) Hauk, P., Stephens, K., McKay, R., Virgile, C. R., Ueda, H., Ostermeier, M., Ryu, K. S., Sintim, H. O., and Bentley, W. E. (2016) Insightful directed evolution of Escherichia coli quorum sensing promoter region of the lsrACDBFG operon: a tool for synthetic biology systems and protein expression. *Nucleic Acids Res. 44*, 10515−10525.
(58) Zhou, K., Qiao, K., Edgar, S., and Stephanopoulos, G. (2015) Distributing a metabolic pathway among a microbial consortium enhances production of natural products. *Nat. Biotechnol. 33*, 377−383.
(59) Jones, J. A., Vernacchio, V. R., Sinkoe, A. L., Collins, S. M., Ibrahim, M. H. A., Lachance, D. M., Hahn, J., and Koffas, M. A. G. (2016) Experimental and computational optimization of an Escherichia coli co-culture for the efficient production of flavonoids. *Metab. Eng. 35*, 55−63.
(60) Dinh, C. V., Chen, X., and Prather, K. L. J. (2020) Development of a quorum-sensing based circuit for control of co-culture population composition in a naringenin production system. *ACS Synth. Biol. 9*, 590−597.
(61) Swift, C. L., Brown, J. L., Seppala, S., and O'Malley, M. A. (2019) Co-cultivation of the anaerobic fungus Anaeromyces robustus with Methanobacterium bryantii enhances transcription of carbohydrate active enzymes. *J. Ind. Microbiol. Biotechnol. 46*, 1427−1433.
(62) Bhagwat, A., Collins, C. H., and Dordick, J. S. (2019) Selective antimicrobial activity of cell lytic enzymes in a bacterial consortium. *Appl. Microbiol. Biotechnol. 103*, 7041−7054.
(63) Gilmore, S. P., Lankiewicz, T. S., Wilken, S. E., Brown, J. L., Sexton, J. A., Henske, J. K., Theodorou, M. K., Valentine, D. L., and O'Malley, M. A. (2019) Top-Down Enrichment Guides in Formation of Synthetic Microbial Consortia for Biomass Degradation. *ACS Synth. Biol. 8*, 2174−2185.
(64) Datsenko, K. A., and Wanner, B. L. (2000) One-step inactivation of chromosomal genes in Escherichia coli K-12 using PCR products. *Proc. Natl. Acad. Sci. U. S. A. 97*, 6640−6645.
(65) Cherepanov, P. P., and Wackernagel, W. (1995) Gene disruption in Escherichia coli: TcR and KmR cassettes with the option of Flp-catalyzed excision of the antibiotic-resistance determinant. *Gene 158*, 9−14.
(66) Sletta, H., Tondervik, A., Hakvag, S., Aune, T. E., Nedal, A., Aune, R., Evensen, G., Valla, S., Ellingsen, T. E., and Brautaset, T. (2007) The presence of N-terminal secretion signal sequences leads to strong stimulation of the total expression levels of three tested medically important proteins during high-cell-density cultivations of Escherichia coli. *Appl. Environ. Microbiol. 73*, 906−912.
(67) Zargar, A., Quan, D. N., and Bentley, W. E. (2016) Enhancing Intercellular Coordination: Rewiring Quorum Sensing Networks for Increased Protein Expression through Autonomous Induction. *ACS Synth. Biol. 5*, 923−928.
(68) Stephens, K., Zargar, A., Emamian, M., Abutaleb, N., Choi, E., Quan, D. N., Payne, G., and Bentley, W. E. (2019) Engineering Escherichia coli for enhanced sensitivity to the autoinducer-2 quorum sensing signal. *Biotechnol. Prog. 35*, No. e2881.
(69) Guzman, L. M., Belin, D., Carson, M. J., and Beckwith, J. (1995) Tight regulation, modulation, and high-level expression by vectors containing the arabinose PBAD promoter. *J. Bacteriol. 177*, 4121−4130.
(70) Ha, J. H., Hauk, P., Cho, K., Eo, Y., Ma, X., Stephens, K., Cha, S., Jeong, M., Suh, J. Y., Sintim, H. O., Bentley, W. E., and Ryu, K. S. (2018) Evidence of link between quorum sensing and sugar metabolism in Escherichia coli revealed via cocrystal structures of LsrK and HPr. *Sci. Adv. 4*, No. eaar7063.
(71) Stephens, K., Pozo, M., Tsao, C. Y., Hauk, P., and Bentley, W. E. (2019) Bacterial co-culture with cell signaling translator and growth controller modules for autonomously regulated culture composition. *Nat. Commun. 10*, 4129.
(72) Servinsky, M. D., Terrell, J. L., Tsao, C. Y., Wu, H. C., Quan, D. N., Zargar, A., Allen, P. C., Byrd, C. M., Sund, C. J., and Bentley, W. E. (2016) Directed assembly of a bacterial quorum. *ISME J. 10*, 158−169.
(73) McKay, R., Hauk, P., Quan, D., and Bentley, W. E. (2018) Development of Cell-Based Sentinels for Nitric Oxide: Ensuring Marker Expression and Unimodality. *ACS Synth. Biol. 7*, 1694−1701.
(74) He, L., Yang, H., Tang, J., Liu, Z., Chen, Y., Lu, B., He, H., Tang, S., Sun, Y., Liu, F., Ding, X., Zhang, Y., Hu, S., and Xia, L. (2019) Intestinal probiotics E. coli Nissle 1917 as a targeted vehicle for delivery of p53 and Tum-5 to solid tumors for cancer therapy. *J. Biol. Eng. 13*, 58.
(75) He, L., Yang, H., Liu, F., Chen, Y., Tang, S., Ji, W., Tang, J., Liu, Z., Sun, Y., Hu, S., Zhang, Y., Liu, X., Huang, W., Ding, X., and Xia, L. (2017) Escherichia coli Nissle 1917 engineered to express Tum-5 can restrain murine melanoma growth. *Oncotarget 8*, 85772−85782.
(76) Isabella, V. M., Ha, B. N., Castillo, M. J., Lubkowicz, D. J., Rowe, S. E., Millet, Y. A., Anderson, C. L., Li, N., Fisher, A. B., West, K. A., Reeder, P. J., Momin, M. M., Bergeron, C. G., Guilmain, S. E.,

https://dx.doi.org/10.1021/acssynbio.0c00179
ACS Synth. Biol. 2020, 9, 2692−2702

Miller, P. F., Kurtz, C. B., and Falb, D. (2018) Development of a synthetic live bacterial therapeutic for the human metabolic disease phenylketonuria. *Nat. Biotechnol. 36*, 857−864.
(77) Duan, F., Curtis, K. L., and March, J. C. (2008) Secretion of insulinotropic proteins by commensal bacteria: rewiring the gut to treat diabetes. *Appl. Environ. Microbiol. 74*, 7437−7438.
(78) Klampfer, L., Zhang, J., and Nimer, S. D. (1999) GM-CSF rescues TF-1 cells from growth factor withdrawal-induced, but not differentiation-induced apoptosis: the role of BCL-2 and MCL-1. *Cytokine+ 11*, 849−855.
(79) Nagai, Y., Garrett, K. P., Ohta, S., Bahrun, U., Kouro, T., Akira, S., Takatsu, K., and Kincade, P. W. (2006) Toll-like receptors on hematopoietic progenitor cells stimulate innate immune system replenishment. *Immunity 24*, 801−812.

https://dx.doi.org/10.1021/acssynbio.0c00179
ACS Synth. Biol. 2020, 9, 2692−2702